Time-Resolved Optical Spectrum Measurement of Multi-Mode Fabry-Perot Laser Diodes

Rongqing Hui, *Senior Member, IEEE*, Youichi Akasaka, *Senior Member, IEEE*, and Paparao Palacharla

***Abstract*— Fabry-Perot (FP) laser diodes usually have multiple longitudinal modes. An optical spectrum analyzer (OSA) is able to measure the average power distribution of the mode structure but cannot detect the dynamics of mode competition which is the origin of the mode partition noise. We demonstrate a time-resolved optical spectrum measurement technique based on frequency-to-time conversion through time gating, chromatic dispersion, and real-time waveform sampling. This allows to investigate the dynamics of mode competition and correlation of relative intensity noises among different FP modes of the diode laser.**

***Index Terms*— Semiconductor lasers, optical communication, Fabry-Perot laser diode, relative intensity noise, mode partition noise, fiber-optics.**

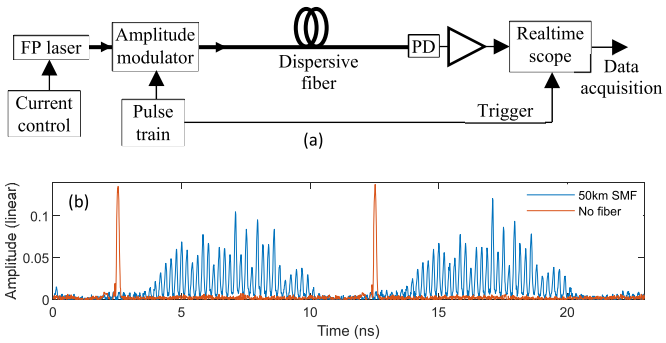

Fig. 1. (a) Experimental setup, and (b) example of waveforms.

I. Introduction

FABRY-PEROT (FP) semiconductor lasers have the advantage of much simpler cavity structure compared to diode lasers with distributed-feedback (DFB), distributed Bragg-reflectors (DBR), and external-cavity structures [1]. Thus, high power diode lasers are mostly made with the FP structure, for example as pump lasers for fiber Raman amplification. However, FP lasers usually have multiple longitudinal modes with the mode spacing $\Delta\lambda$ inversely proportional to the cavity length L, as $\Delta\lambda = \lambda^2/(2nL)$, where λ is the center wavelength of the laser and n is the effective refractive index [2]. A typical FP laser diode can have tens of longitudinal modes. When operating above lasing threshold, these modes compete for the optical gain supported by the carrier density, especially when the material gain has a homogeneous broadening mechanism [1]. Mode competition and mode partition noise in FP laser diodes have been extensively investigated in the early days of optical communications [3], [4], [5], [6], [7], and more recently for applications as low-RIN Raman pump lasers [8] and optical frequency combs [9], [10]. Mode partition noise, arises from the dynamics of mode competition, creates not only the relative intensity noise (RIN), but also wavelength fluctuation of the laser emission.

Manuscript received 19 June 2022; revised 30 September 2022; accepted 19 October 2022. Date of publication 25 October 2022; date of current version 7 December 2022. This work was supported in part by the U.S. National Science Foundation under Grant CNS-1956137. *(Corresponding author: Rongqing Hui.)*

Rongqing Hui is with the Department of Electrical Engineering and Computer Science, University of Kansas, Lawrence, KS 66045 USA (e-mail: rhui@ku.edu).

Youichi Akasaka and Paparao Palacharla are with Fujitsu Network Communications Inc., Richardson, TX 75082 USA (e-mail: youichi.akasaka@fujitsu.com; paparao.palacharla@fujitsu.com).

Color versions of one or more figures in this letter are available at https://doi.org/10.1109/LPT.2022.3216751.

Digital Object Identifier 10.1109/LPT.2022.3216751

Characterizing the dynamics of mode competition requires the simultaneous power measurement of individual spectral lines across the laser spectrum. An optical spectrum analyzer (OSA) can be used conveniently to measure the optical spectrum and to characterize the mode structure such as the number of modes and wavelength spacing between adjacent modes of a laser diode. However, the optical spectrum measured by an OSA is the averaged spectrum [11] because of the relatively slow spectral scanning rate on the order of a second, and thus, the dynamics of mode competition in a FP laser cannot be characterized. Different FP modes from a laser diode can be separated by a WDM demultiplexer (DEMUX) followed by parallel detection [7]. But this requires the DEMUX to exactly match the free-spectral range (FSR) of the FP laser emission, and multiple photodiodes each followed by a pre-amplifier and data acquisition need to be used, which is not practical when the number of spectral lines is large.

In this letter we present a time-resolved optical spectrum measurement technique based on frequency-to-time conversion through time gating, chromatic dispersion, and digital waveform acquisition with a real-time oscilloscope. This simple technique allows the characterization of mode partitioning dynamics of FP diode lasers, as well as the correlation of power fluctuations among different spectral lines. Two FP diode lasers made of semiconductor materials of bulk and quantum-well structures, respectively, are used as examples to demonstrate the measurement technique. The former has much stronger mode partition noise than the later, and we show that their mode partition dynamics are also very different.

II. Experimental Setup

Fig. 1(a) shows the measurement setup. The output of a FP diode laser is modulated by an electro-optic intensity modulator into a pulse train with a pulse width ΔT and a pulse repetition time T_R. This optical pulse train is sent to

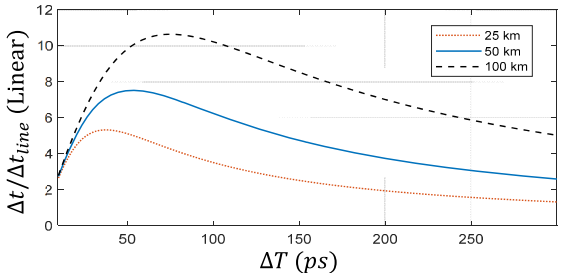

Fig. 2. Calculated ratio between mode separation and pulse width at the fiber output based on $\Delta\lambda = 1nm$, $D = 16ps/nm/km$, and fiber lengths of $L = 25$km, 50km and 100km, respectively.

a dispersive optical fiber and detected by a direct-detection optical receiver. The waveform is then digitized and recorded by a real-time oscilloscope for signal analysis. Chromatic dispersion in the fiber creates differential time walk-off between different spectral lines of the FP laser emission. For a fiber with length L and a dispersion parameter D at the lasing wavelength, time separation between adjacent laser modes will be $\Delta t = D \cdot L \cdot \Delta\lambda$, with $\Delta\lambda$ the mode spacing [11]. Fig. 1(b) illustrates typical waveforms recorded at the receiver for a system without and with fiber, respectively. Without a fiber in the system, the modulated pulse train with 10ns repetition time and 100ps pulse width is directly measured by the receiver. After inserting an optical fiber, the modulated pulses carried by adjacent laser modes are separated by Δt at the receiver, so that the optical spectrum is linearly translated to the time domain with a wavelength to time conversion efficiency $\delta t/\delta\lambda = D \cdot L$. As the pulse train is repetitive, the spectral scanning is repeated every 10ns in this case, which is many orders of magnitude faster than that with a conventional OSA.

In order to clearly separate different spectral lines in a FP laser spectrum, the figure of merit is the ratio between the mode separation Δt and the width of each spectral line Δt_{line} in the time domain, which are determined by the pulse width of modulation and the fiber dispersion. Fig. 2 shows calculated $\Delta t/\Delta t_{line}$ as the function of pulse width ΔT at the fiber input for 3 different fiber lengths, where $\Delta t_{line} = \frac{\lambda^2}{\pi c}\frac{ln(4)}{\Delta T} D \cdot L$ is used, assuming ΔT is the full width at half maximum (FWHM) of a Gaussian pulse [2]. Decreasing ΔT will reduce the pulse width Δt_{line} at the fiber output. But when ΔT is too narrow, the spectral width will be broadened which broadens the temporal width of each laser mode at the fiber output due to chromatic dispersion and reducing the ratio $\Delta t/\Delta t_{line}$. 50ps to 100ps pulse width is generally appropriate at the fiber input for this measurement. The generation of external modulation with a pulse width on the order of 100ps can be accomplished with an electro-optic modulator typically used for 10Gb/s fiber-optic communication systems with about 40ps rise/fall time.

III. Results and Discussion

The 1st device we have measured is an uncooled low-cost FP laser diode operating in the 1550nm wavelength with mode spacing $\Delta\lambda = 1.14nm$. This laser, produced in 1980s, is made of bulk semiconductor material with a maximum output optical power of 2mW. The measurement uses a pulse repetition time of $T_R = 20ns$, a pulse width of $\Delta T = 100ps$,

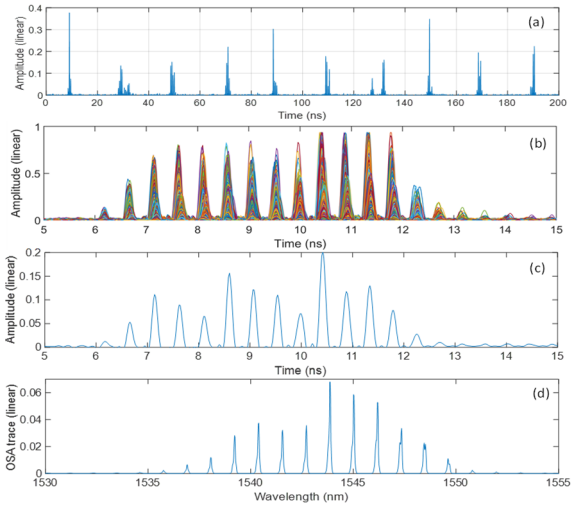

Fig. 3. Figure 3. (a): 10 consecutive measurements of laser emission spectrum, (b): a collection of 2000 measurements folded into a single 10ns time frame, (c) average spectrum of the 2000 measurements, and (d) optical spectrum measured by an OSA.

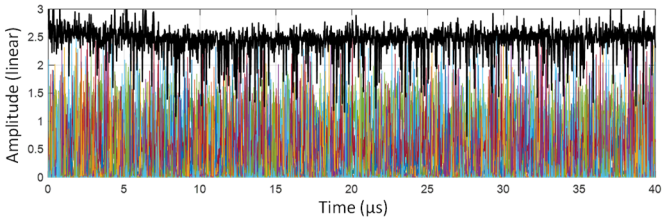

Fig. 4. Power of each individual mode (in different colors), and the total power (black bold) as the function of time.

and $L = 24.2km$ standard single mode fiber (SMF) with $D = 16.4ps/nm/km$ at the signal wavelength. An EDFA is used before the receiver to improve the signal to noise ratio (SNR) of the measured waveform. Fig.3 (a) shows an example of 10 consecutive measurements of laser spectrum. Because of the homogeneous broadening of the material gain, mode competition is intense, and often there is only a single dominant spectral line in the laser emission. Fig.3(b) is the collection of 2000 consecutive measurements, which shows the general mode spectrum of this laser. The average of these 2000 measurements is shown in Fig.3(c) which is equivalent to an averaged optical spectrum indicating the statistic distribution of optical power in different modes over a $40\mu s$ integration time. In this measurement, the 10ns time window shown in Fig.3(b) and (c) is equivalent to a spectral window of $\delta\lambda = 10^{-8}/(D \cdot L) \approx 25.2nm$. For comparison, Fig.3 (d) shows the optical spectrum measured by a bench-top grating-based OSA.

To understand mode competition dynamics, the power of each spectral line in Fig.3(b) can be separately extracted digitally as a function of time, as shown in Fig. 4. This is equivalent to measuring the power of each mode at 50MS/s sampling rate. Fig.4 shows tremendous power fluctuation of each individual mode due to mode competition in a homogeneously broadening laser gain medium, which has been extensively studied in the literature. The total power, including all the modes, represented by the bold black line in Fig.4 has less intensity noise compared to each individual mode, but still

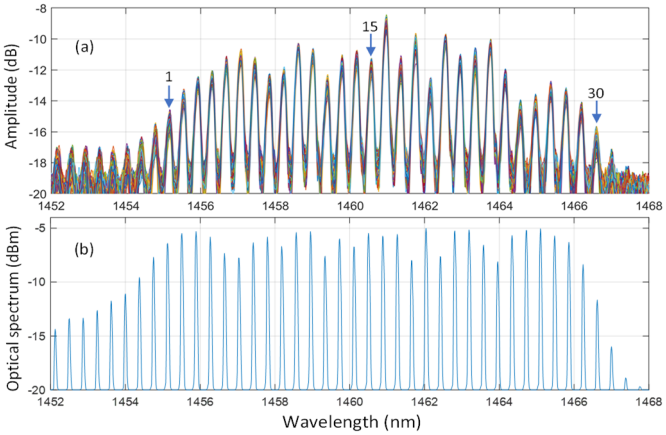

Fig. 5. (a) A collection of 1200 measurement folded into a single 10ns time frame, and the horizontal axis is then linearly converted into a wavelength scale, (b) optical spectrum measured by an OSA.

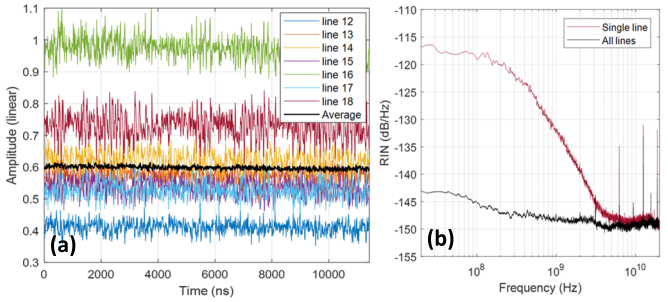

Fig. 6. (a) Measured optical power of 7 individual spectral lines (colored), and the average of 10 spectral lines (bulk black) in the middle part of the laser spectrum, as the function of time. (b) measured RIN of total laser power (black) and the power of the 16th spectral line.

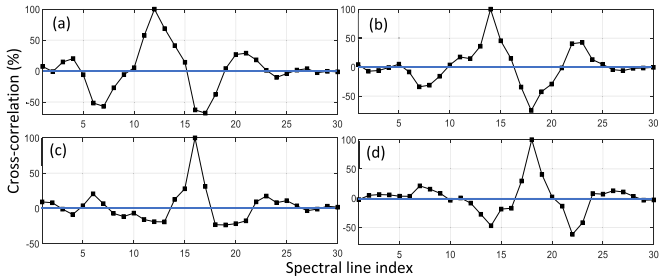

Fig. 7. Cross-correlation of power fluctuations of spectral lines 12 (a), 14 (b), 16 (c) and 18 (d) with all other spectral lines. Autocorrelation of spectral lines 12, 14, 16 and 18 are used to normalize the cross-correlation values in (a), (b), (c) and (d).

has a very high RIN level on the order of −70dB/Hz. This RIN was calculated based on $RIN\,(\omega) = S_P\,(\omega)\,/P_{ele,ave}$, where $S_P\,(\omega)$ is the power spectral density obtained from the Fourier transform of the measured time-domain waveform shown in Fig.4, and $P_{ele,ave}$ is the average power [11, Sec.3.1.1]. Because of the 20ns repetition time of the pulse train which samples the waveform, the maximum frequency of RIN is limited to about 25MHz.

In recent years, quantum well structures in diode lasers have shown to have reduced linewidth enhancement factors and partially inhomogeneous broadening of optical gain due to the tight spatial confinement of carrier distribution. As a result, mode competition can be greatly reduced to allow simultaneous emission of relatively stable multiple spectral lines from a FP laser diode. The overall RIN can also be dramatically reduced compared to using bulk semiconductor materials.

The 2nd device used to demonstrate the measurement technique is a high-power FP laser diode emitting at 1460nm wavelength designed for distributed Raman pumping in fiber systems. The laser is made of quantum-well structure, and the emission is coupled into a SMF via an optical isolator, with 250mW power from the fiber pigtail at 800mA bias current. The mode spacing of this laser is $\Delta\lambda \approx 0.39nm$. In order to avoid fiber nonlinear effect, the optical power is attenuated to about 10mW before sending into the intensity modulator to create the optical pulse train. 50km standard SMF is used with accumulated dispersion of $D \cdot L = 538ps/nm$ at the 1460nm wavelength. Because an EDFA does not cover this wavelength window, distributed Raman amplification is used in the experiment to increase the signal optical power at the receiver by using a high power 1365nm backward Raman pumping into the 50km fiber. This measurement used pulse repetition time $T_R = 10ns$, and pulse width $\Delta T = 100ps$.

Fig.5(a) shows the collection of 1200 consecutive measurements folded into a single 10ns time window, and the horizontal axis has been converted into wavelength scale based on a conversion factor of $\delta\lambda/\delta t = (D \cdot L)^{-1} = 1.859nm/ns$. This converted optical spectrum is similar to the spectrum measured by a grating-based OSA shown in Fig. 5(b). In comparison to Fig.3(b), Fig.5(a) shows much more stable amplitude of each laser mode. To further investigate the mode dynamics, we have marked 30 major spectral lines as shown in Fig.5(a) and measured the power of each spectral line as the function of time. Fig.6(a) shows the power of 6 spectral lines in the middle of the spectrum. This is equivalent to measuring the power variation of each laser mode as the function of time at a 100MS/s sampling rate. Although the power of each spectral line fluctuates around its mean value, the variance is much smaller compared to those shown in Fig.4. The bold black line in Fig. 6(a) is the average power of spectral lines 10 to 20 indicated in Fig.5(a), and the variance is much smaller than that of any individual spectral line. The black curve in Figure 6(b) shows the measured RIN of this laser based on the total power including all the modes, and the maximum RIN level is less than −140dB/Hz. The magenta curve in Fig. 6(b) is the RIN measured with a single spectral line (line 16 in this case) selected by a narrowband optical filter, and the RIN level is slightly higher than −120dB/Hz at low frequencies. To show high frequency components of RIN, the spectra shown in Fig.6(b) were measured directly at the laser output with 100GS/s sampling rate following a DC-coupled photodetector. The conversion from time domain waveforms to the RIN spectra was the same as described in [11, Sec.3.1]. Note that this is about 25dB lower than that of a recently reported result of single-section quantum-well laser [9]. Part of the reason for this difference may be attributed to the high-power level of the laser used in our experiment which is more than 10 times higher that used in [9].

The unique advantage of this measurement technique is that the power levels of different spectral lines are measured simultaneously as the function of time. This allows

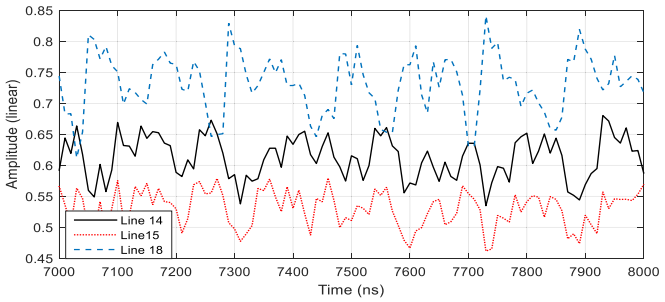

Fig. 8. Power of each individual modes 14 (solid line), 15 (dotted line) and 18 (dashed line) as the function of time.

the correlation measurement of intensity fluctuations among different laser modes which is useful for further investigation and understanding of mode partition and competition mechanisms. Fig.7(a) shows the cross-correlation of power fluctuation between spectral line 12 and all other spectral lines, in which the values are normalized by the autocorrelation of line 12. This figure indicates that power fluctuation of spectral line 12 is predominately in-phase (positive cross-correlation) with that of its immediate neighboring spectral lines, and anti-phase (negative cross-correlation) with spectral lines 4 - 5 FSRs away. Cross-correlation gradually diminishes for spectral lines ± 10 FRSs away. Similarly, Fig.7 (b) – (d) show cross-correlations of power fluctuations of spectral lines 14, 16, and 18 with all other spectral lines, respectively, and the general characteristics are similar to those described for Fig.7(a).

To further illustrate the correlation of intensity noises among different spectral lines, Fig. 8 shows a short section of measured power fluctuations of spectral lines 14, 15, and 18 as the function of time. This figure clearly shows that power fluctuations of spectral lines 14 and 15 are predominately in-phase, while they are anti-phase with spectral line 18. As the mode spacing of this laser is 0.39nm, or approximately 55GHz in frequency, it appears that within a bandwidth of approximately 100GHz, the spectral lines are teamed up to compete for powers against spectral lines approximately 200GHz away. The specific mechanism is not very clear at this point, and still requires further investigation with more device details, but it should be related to the intra sub-band carrier dynamics inside the quantum-well structure [10].

From an application point of view, the high-power quantum-well lasers discussed here are designed for distributed Raman amplification in fiber-optic systems. When used for forward Raman pumping, the pump laser must have low RIN to avoid RIN transfer from the pump laser to the RIN and the phase noise of the signals it amplifies. While the RIN of the total power (including all the modes) of this laser is less than -140dB/Hz, the RIN of an individual FP mode can be as high as -120dB/Hz in the low frequency region, and the dynamic power shift among different spectral lines may affect the stability of the Raman gain spectrum. However, as the correlation bandwidth of mode competition is on the order of 200GHz, or about 1.5nm as shown in Fig.7, which is much smaller than the approximately 10nm Raman amplification bandwidth in silica fibers, the impact of mode competition should not be a major concern. Nevertheless, a systemic investigation with more laser samples may still be necessary to draw an informative conclusive.

In recent years, mode-locked laser diodes based on quantum-dots [12], [13] and quantum-dash [14], [15] have been demonstrated to generate optical frequency combs, and they are promising for applications in optical communications. The measurement technique demonstrated here can be useful also to characterize these frequency combs in terms of the stability and dynamics of different spectral lines.

IV. Conclusion

We have demonstrated a simple technique to perform time-resolved optical spectrum measurement based on frequency-to-time conversion through time gating, chromatic dispersion, and real-time digital waveform sampling. With this technique, power fluctuations of individual spectral lines from a FP laser emission can be measured simultaneously. As application examples, we have investigated the dynamics of mode competition and cross-correlation of intensity noises among different FP modes of two diode lasers of different structures. We show that for a diode laser made of bulk semiconductor material, power competition among FP modes is significant, resulting in very high RIN of the total power. On the other hand, a high-power diode laser based on multiple quantum-well structure exhibits much less mode competition and with clear cross-correlation between adjacent modes.

References

[1] P. A. Govind and N. K. Dutta, *Semiconductor Lasers*, 2nd ed. Berlin, Germany: Springer, 2013.
[2] H. Rongqing, *Introduction to Fiber-Optic Communications*. New York, NY, USA: Academic, 2019.
[3] P.-L. Liu and K. Ogawa, "Statistical measurements as a way to study mode partition in injection lasers," *J. Lightw. Technol.*, vol. LT-2, no. 1, pp. 44–48, Feb. 1984.
[4] M. Ohtsu and Y. Teramachi, "Analyses of mode partition and mode hopping in semiconductor lasers," *IEEE J. Quantum Electron.*, vol. 25, no. 1, pp. 31–38, Jan. 1989.
[5] R. Wentworth, G. E. Bodeep, and T. E. Darcie, "Laser mode partition noise in lightwave systems using dispersive optical fiber," *J. Lightw. Technol.*, vol. 10, no. 1, pp. 84–89, Jan. 1992.
[6] M. R. Alalusi and B. B. Darling, "Effects of nonlinear gain on mode-hopping in semiconductor laser diodes," *IEEE J. Quantum Electron.*, vol. 31, no. 7, pp. 1181–1192, Jul. 1995.
[7] R. G. Gray and R. Roy, "Bistability and mode hopping in a semiconductor laser," *J. Opt. Soc. Amer. B, Opt. Phys.*, vol. 8, pp. 632–638, Mar. 1991.
[8] G. Bolognini, S. Faralli, A. Chiuchiarelli, F. Falconi, and F. D. Pasquale, "High-power and low-RIN lasers for advanced first- and higher order Raman copumping," *IEEE Photon. Technol. Lett.*, vol. 18, no. 15, pp. 1591–1593, Aug. 21, 2006.
[9] C. Calò et al., "Single-section quantum well mode-locked laser for 400 Gb/s SSB-OFDM transmission," *Opt. Exp.*, vol. 23, no. 20, pp. 26442–26449, 2015.
[10] M. Dong, N. M. Mangan, J. N. Kutz, S. T. Cundiff, and H. G. Winful, "Traveling wave model for frequency comb generation in single-section quantum well diode lasers," *IEEE J. Quantum Electron.*, vol. 53, no. 6, pp. 1–11, Dec. 2017.
[11] R. Hui and M. O'Sullivan, *Fiber Optic Measurement Techniques*. New York, NY, USA: Academic, 2009.
[12] Z. Lu et al., "InAs/InP quantum dash semiconductor coherent comb lasers and their applications in optical networks," *J. Lightw. Technol.*, vol. 39, no. 12, pp. 3751–3760, Jun. 15, 2021.
[13] Z. Lu, J. Liu, L. Mao, C.-Y. Song, J. Weber, and P. Poole, "12.032 Tbit/s coherent transmission using an ultra-narrow linewidth qantum dot 34.46-GHz C-band coherent comb laser," *Proc. SPIE*, vol. 10947, pp. 116–122, Feb. 2019.
[14] M. Z. M. Khan, "Towards InAs/InP quantum-dash laser-based ultra-high capacity heterogeneous optical networks: A review," *IEEE Access*, vol. 10, pp. 9960–9988, 2022.
[15] J. N. Kemal et al., "Coherent WDM transmission using quantum-dash mode-locked laser diodes as multi-wavelength source and local oscillator," *Opt. Exp.*, vol. 27, pp. 31164–31175, Oct. 2019.